A simple yet effective a posteriori estimator for classical mixed approximation of Stokes equations

Liao, Qifeng and Silvester, David

2010

Manchester Institute for Mathematical Sciences

School of Mathematics

The University of Manchester

A simple yet effective a posteriori estimator for classical mixed approximation of Stokes equations

Qifeng Liao, David Silvester *

School of Mathematics, University of Manchester, Manchester, M13 9PL, United Kingdom

A R T I C L E   I N F O

A B S T R A C T

The implementation of quadratic velocity, linear pressure finite element approximation methods for the steady-state incompressible (Navier–)Stokes equations is addressed in this work. Three types of a posteriori error indicator are introduced and are shown to give global error estimates that are equivalent to the true discretisation error. Computational results suggest that the solution of local Poisson problems provides a cost-effective error estimation strategy, both from the perspective of accurate estimation of the global error and for the purpose of selecting elements for refinement within a contemporary self-adaptive refinement algorithm.

© 2010 Published by Elsevier B.V. on behalf of IMACS.

1. Introduction

During the last two decades there has been a rapid development in practical a posteriori error estimation techniques for elliptic PDEs. This explosion in interest has been driven by the underlying need to increase the reliability and efficiency of finite element software for solving such problems. The books by Ainsworth and Oden [3] and Verfürth [18] give a general overview. In the specific case of the Stokes and Navier–Stokes equations governing the steady flow of a viscous incompressible fluid, the work of Bank and Welfert [4] and of Verfürth [17] laid the basic foundation for the mathematical analysis of practical methods. The "local Poisson problem" error estimation methodology that we adopt herein was introduced by Ainsworth and Oden in [2] and is strongly featured in the book of Elman et al. [10, Section 5.4.2].

The pioneering a posteriori error estimation techniques for incompressible flow were built around stable P_1–P_1 (linear velocity, continuous linear pressure) mixed approximation, using either bubble terms (i.e. the mini-element, see e.g. [5, p. 153]), or a macroelement definition of the pressure (see e.g. [5, p. 152]) to guarantee stability. The aim of this paper is to provide simple and effective error estimation techniques for higher order stable mixed approximations: in particular Q_2–P_{-1} (biquadratic velocity, discontinuous linear pressure, see [10, p. 234]), and the Crouzeix-Raviart P_{2*}–P_{-1} approximation (superquadratic velocity, discontinuous linear pressure, see [10, p. 248]). Although we restrict attention to two-dimensional approximation throughout, the extension of our approach to three-dimensional Q_2–P_{-1} or P_{2*}–P_{-1} approximation using bricks or tetrahedra is completely straightforward. The paper builds on our earlier work [14] where we considered error estimation and adaptivity in the case of unstable P_1–P_0 (linear velocity, constant pressure) approximation in two dimensions. Finally, although our focus here is on the simplest case of Stokes flow, our methodology can be readily extended to the Navier–Stokes equations. See [10, Section 7.4.2] for further details.

An outline of the paper is as follows. In the next section we review the notion of mixed approximation of the Stokes equations. We present a theoretical analysis of three a posteriori error estimation strategies for Q_2–P_{-1} mixed approximation in Section 3. Specifically, three alternative error estimators are shown to be equivalent to the discretisation error.

---

* Corresponding author.
   E-mail addresses: Qifeng.Liao@postgrad.manchester.ac.uk (Q. Liao), d.silvester@manchester.ac.uk (D. Silvester).

Some numerical results are presented in Section 4. Here the efficiency and reliability of the Poisson problem estimator is compared with the popular Z–Z error indicator originally introduced by Zienkiewicz and Zhu [19]. Some conclusions are given in Section 5.

2. Mathematical setting

We will consider the simplest possible model of viscous incompressible flow in an idealized, bounded, connected domain in $\mathbb{R}^2$:

$$-\nabla^2 \vec{u} + \nabla p = 0 \quad \text{in } \Omega, \tag{1}$$

$$\nabla \cdot \vec{u} = 0 \quad \text{in } \Omega, \tag{2}$$

$$\vec{u} = \vec{w} \quad \text{on } \partial\Omega_D, \tag{3}$$

$$\frac{\partial \vec{u}}{\partial n} - \vec{n} p = 0 \quad \text{on } \partial\Omega_N. \tag{4}$$

We also assume that Ω has a polygonal boundary $\partial\Omega = \partial\Omega_D \cup \partial\Omega_N$, $\partial\Omega_D \cap \partial\Omega_N = \emptyset$, so that $\vec{n}$ is the usual outward-pointing normal. The vector field $\vec{u}$ is the velocity of the flow and the scalar variable p represents the pressure. Our mathematical model is very simple: the velocity is given on inflow and fixed parts of the boundary $\partial\Omega_D$, and there is a zero flux condition that applies on $\partial\Omega_N$ typically representing an outflow. The boundary data $\vec{w}$ is assumed to be in the space $H^{1/2}(\partial\Omega_D)^2 := \{\vec{v} | \vec{v} = \vec{u}|_{\partial\Omega_D}, \vec{u} \in H^1(\Omega)^2\}$. For convenience, the boundary data $\vec{w}$ will also be assumed to be a polynomial with order at most two—this will ensure that there is no error incurred in approximating the boundary condition on $\partial\Omega_D$.

In the following we use the function space notation: $\boldsymbol{H}_E^1 := \{\vec{u} \in H^1(\Omega)^2 \mid \vec{u} = \vec{w} \text{ on } \partial\Omega_D\}$ and $\boldsymbol{H}_{E_0}^1 := \{\vec{u} \in H^1(\Omega)^2 \mid \vec{u} = \vec{0} \text{ on } \partial\Omega_D\}$. Moreover, when $\int_{\Omega_N} ds > 0$, the pressure space is defined by $\boldsymbol{P} := L^2(\Omega)$, whereas when $\int_{\Omega_N} ds = 0$, the pressure space is $\boldsymbol{P} := L_0^2(\Omega)$ (all the functions have mean zero). The latter case is also referred to as an *enclosed* flow problem.

The weak formulation of (1)–(4) is: find $\vec{u} \in \boldsymbol{H}_E^1$ and $p \in \boldsymbol{P}$ such that

$$\int_\Omega \nabla \vec{u} : \nabla \vec{v} - \int_\Omega p \nabla \cdot \vec{v} = 0 \quad \forall \vec{v} \in \boldsymbol{H}_{E_0}^1, \tag{5}$$

$$\int_\Omega q \nabla \cdot \vec{u} = 0 \quad \forall q \in \boldsymbol{P}. \tag{6}$$

As is well known, see Girault and Raviart's book [11, pp. 59–61], a sufficient condition for the existence and uniqueness of a solution satisfying (5)–(6) is the continuous inf-sup condition that is stated below.

Definition 2.1. Continuous inf-sup condition: there exists a positive constant γ dependent on the shape of the domain Ω such that,

$$\inf_{0 \neq q \in \boldsymbol{P}} \sup_{\vec{0} \neq \vec{v} \in \boldsymbol{H}_{E_0}^1} \frac{|(q, \nabla \cdot \vec{v})|}{|\vec{v}|_1 \|q\|_0} \geqslant \gamma. \tag{7}$$

In the sequel, this continuous inf-sup condition will be assumed to be satisfied. To the authors' knowledge, establishing this continuous inf-sup condition for an arbitrary domain Ω with a natural outflow condition (4) is an open problem. For enclosed flow problems there are some theoretical results for special domain types. For example, Chizhonkov and Olshanskii [6] prove that, for a channel domain, the continuous inf-sup constant γ decreases in proportion to the length of channel. Herein, we assume that the domain Ω is fixed, so the degeneration of the continuous inf-sup constant is not an issue.

An immediate consequence of the stability bound (7) is the "$\mathfrak{B}$-stability bound" given below. For a proof see [10, Lemma 5.2].

Proposition 2.2. $\mathfrak{B}$-*stability*: *working with the "big" bilinear form* $\mathfrak{B} : (\boldsymbol{H}^1, \boldsymbol{P}) \times (\boldsymbol{H}^1, \boldsymbol{P}) \to \mathbb{R}$ *so that*

$$\mathfrak{B}\big((\vec{u}, p); (\vec{v}, q)\big) = (\nabla \vec{u}, \nabla \vec{v}) - (p, \nabla \cdot \vec{v}) - (q, \nabla \cdot \vec{u}), \tag{8}$$

then, for all $(\vec{w}, s) \in \boldsymbol{H}_{E_0}^1 \times \boldsymbol{P}$, *we have that*

$$\sup_{(\vec{v},q) \in \boldsymbol{H}_{E_0}^1 \times \boldsymbol{P}} \frac{\mathfrak{B}((\vec{w}, s); (\vec{v}, q))}{|\vec{v}|_{1,\Omega} + \|q\|_{0,\Omega}} \geqslant \gamma_D \big(|\vec{w}|_{1,\Omega} + \|s\|_{0,\Omega}\big), \tag{9}$$

where γ_D *depends only on the shape of the domain* Ω.
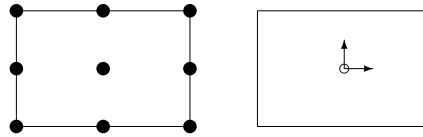
Fig. 1. Q_2–P_{-1} element (● velocity node; ○ pressure; $\overset{\uparrow}{\to}$ pressure derivative).

2.1. Finite element approximation

Mixed finite element approximation of (5)–(6) is obtained by taking finite-dimensional subspaces X_E^h to approximate $\boldsymbol{H}_E^1$, X_0^h to approximate $\boldsymbol{H}_{E_0}^1$ and M^h to approximate $\boldsymbol{P}$. Thus, the Galerkin formulation is: find $\vec{u}_h \in X_E^h$ and $p_h \in M^h$ such that,

$$\int_\Omega \nabla \vec{u}_h : \nabla \vec{v}_h - \int_\Omega p_h \nabla \cdot \vec{v}_h = 0 \quad \forall \vec{v}_h \in X_0^h, \tag{10}$$

$$\int_\Omega q_h \nabla \cdot \vec{u}_h = 0 \quad \forall q_h \in M^h. \tag{11}$$

Note that the approximation velocity space X_E^h is obtained from the test space X_0^h:

$$X_E^h = \left(\vec{u} \mid \vec{u} = \sum_{j=1}^{n_u} a_j \vec{\phi}_j + \sum_{j=n_u+1}^{n_u+n_\partial} a_j \vec{\phi}_j \right), \tag{12}$$

with coefficients $a_j \in \mathbb{R}$ and associated basis functions $\{\vec{\phi}_j\}_{j=1}^{n_u}$ that span X_0^h. The additional coefficients $a_j : j = n_u + 1, \ldots, n_u + n_\partial$ are associated with the Lagrange interpolation of the boundary data $\vec{w}$ on $\partial\Omega_D$. Collecting the coefficients $\{a_j\}_{j=1}^{n_u}$ into a vector $\mathbf{u}$ and associating a vector $\mathbf{p} \in \mathbb{R}^{n_p}$ with the coefficients in the expansion of p_h leads to a characteristic system of algebraic equations:

$$\begin{bmatrix} A & B^T \\ B & 0 \end{bmatrix} \begin{bmatrix} \mathbf{u} \\ \mathbf{p} \end{bmatrix} = \begin{bmatrix} \mathbf{f} \\ \mathbf{g} \end{bmatrix}. \tag{13}$$

The finite-dimensional spaces X_0^h and M^h are related to the partitioning T_h of Ω. In this work, we will focus on the simplest case of regular rectangular meshes—which implies that the aspect ratio of each rectangle in the mesh is bounded—and we concentrate on the Q_2–P_{-1} approximation that has the degrees of freedom shown in Fig. 1. This velocity–pressure combination is regarded by practitioners as being one of the most cost-effective approaches in two dimensions.

One necessary condition for the mixed approximation is that the associated "saddle-point" system (13) is solvable. Analogously to the continuous situation, a sufficient condition for the unique solvability of (13) is a (discrete-) inf-sup condition.

Definition 2.3. Discrete inf-sup condition: there exists a positive constant γ_* (called the inf-sup constant) independent of h, such that

$$\min_{0 \neq q_h \in M^h} \max_{0 \neq \vec{v}_h \in X_0^h} \frac{|(q_h, \nabla \cdot \vec{v}_h)|}{|\vec{v}_h|_1 \|q_h\|_0} \geqslant \gamma_h \geqslant \gamma_* > 0. \tag{14}$$

As discussed in [10, Section 5.5], for any given grid, γ_h is just the square root of the smallest nonzero eigenvalue λ of the following generalized eigenvalue problem,

$$BA^{-1}B^T \mathbf{x} = \lambda Q \mathbf{x}, \tag{15}$$

where the matrices B, A are those given in (13), and Q is the Grammian matrix associated with the basis functions spanning the pressure approximation space M^h. The stability of Q_2–P_{-1} approximation was first established by Stenberg in [16]. In the case of enclosed flow, $\partial\Omega_N = \emptyset$, computational results presented in [10, Table 5.6] suggest that the inf-sup constant associated with Q_2–P_{-1} approximation on uniform square grids satisfies $\gamma_* > 1/5$.

We let $(\vec{u}, p)$ denote the solution of (5)–(6) and let $(\vec{u}_h, p_h)$ denote the solution of (10)–(11) with Q_2–P_{-1} approximation on a rectangular subdivision T_h. Our aim is to estimate the velocity and the pressure errors

$$\vec{e} = \vec{u} - \vec{u}_h, \qquad \epsilon = p - p_h, \tag{16}$$

by post-processing the computed solution $(\vec{u}_h, p_h)$. To make progress towards this aim, some notation is needed. For any $T \in T_h$, ω_T is the set of rectangles sharing at least one edge with element T, while $\tilde{\omega}_T$ is the set of rectangles sharing at

least one vertex with T. Also, for an element edge E, ω_E denotes the union of rectangles sharing E, while $\tilde{\omega}_E$ is the set of rectangles sharing at least one vertex with E. Next, ∂T is the set of the four edges of T. Moreover, $\varepsilon_{h,\Omega}$ is the set of element edges inside of Ω, $\varepsilon_{h,D}$ is the set of element edges on the boundary $\partial\Omega_D$ and $\varepsilon_{h,N}$ is the set of element edges on the boundary $\partial\Omega_N$. We also follow established convention and let C and c denote generic constants which are independent of the mesh size, the domain Ω, and the solution $(\vec{u}, p)$. Such constants could depend on the aspect ratio of the elements in T_h.

If an error estimator η is to be useful then an important factor is the requirement that it should be cheap to compute—as a rule of thumb, the computational work should scale linearly as the number of elements is increased—yet there should be guaranteed accuracy in the sense that the estimated global error should give an upper bound on the exact error, so that

$$|\vec{e}|_{1,\Omega} + \|\epsilon\|_{0,\Omega} \leqslant C_\Omega \eta. \tag{17}$$

Here the generic constant C_Ω is independent of the mesh size and the exact solution but may depend on the domain and the element aspect ratio. If, in addition to satisfying (17), the associated *local* (element-) error estimator η_T (with $\eta = \sqrt{\sum_{T \in T_h} \eta_T^2}$) provides a lower bound for the exact local error

$$\eta_T \leqslant C_\Omega \left(\sum_{T' \in \omega_T} \{ |\vec{e}|_{1,T'}^2 + \|\epsilon\|_{0,T'}^2 \} \right)^{1/2}, \tag{18}$$

then the estimator η_T is likely to be effective if it is used to drive an adaptive refinement process. In the next section we will introduce three alternative estimators and show that each satisfies the requirements (17) and (18).

3. Analysis of estimators

We begin this section by summarising some standard results that will prove to be useful. First, so-called bubble functions on the reference element $\tilde{T} = (0, 1) \times (0, 1)$ are defined as follows:

$$b_{\tilde{T}} = 2^4 x(1 - x) y(1 - y),$$
$$b_{\tilde{E}_1, \tilde{T}} = 2^2 x(1 - x)(1 - y),$$
$$b_{\tilde{E}_2, \tilde{T}} = 2^2 y(1 - y)x,$$
$$b_{\tilde{E}_3, \tilde{T}} = 2^2 x(1 - x)y,$$
$$b_{\tilde{E}_4, \tilde{T}} = 2^2 y(1 - y)(1 - x).$$

Here $b_{\tilde{T}}$ is the reference *element* bubble function, and $b_{\tilde{E}_i, \tilde{T}}$, $i = 1:4$ are reference *edge* bubble functions. For any $T \in T_h$, the *element* bubble function is $b_T = b_{\tilde{T}} \circ F_T$ and the element *edge* bubble function is $b_{E_i, T} = b_{\tilde{E}_i, \tilde{T}} \circ F_T$, where F_T is the affine map from $\tilde{T}$ to T. For an interior edge $E \in \varepsilon_{h,\Omega}$ and $E = \overline{T_1} \cap \overline{T_2}$, b_E is defined as follows,

$$b_E = \begin{cases} b_{E,T_1} & \text{in } \overline{T_1}, \\ b_{E,T_2} & \text{in } \overline{T_2}, \\ 0 & \text{in } \Omega \setminus (\overline{T_1} \cup \overline{T_2}). \end{cases} \tag{19}$$

For a boundary edge $E \in \varepsilon_{h,D} \cup \varepsilon_{h,N}$, $b_E = b_{E,T}$, where T is the rectangle such that $E \in \partial T$. With these bubble functions, Creusé et al. [8, Lemma 4.1] established the following lemma.

Lemma 3.1. *Inverse inequalities: let T be an arbitrary rectangle in T_h and $E \in \partial T$. For any $\vec{v}_T \in P_{k_0}(T)$ and $\vec{v}_E \in P_{k_1}(E)$, the following inequalities hold,*

$$c_k \|\vec{v}_T\|_{0,T} \leqslant \|\vec{v}_T b_T^{1/2}\|_{0,T} \leqslant C_k \|\vec{v}_T\|_{0,T}, \tag{20}$$

$$|\vec{v}_T b_T|_{1,T} \leqslant C_k h_T^{-1} \|\vec{v}_T\|_{0,T}, \tag{21}$$

$$c_k \|\vec{v}_E\|_{0,E} \leqslant \|\vec{v}_E b_E^{1/2}\|_{0,E} \leqslant C_k \|\vec{v}_E\|_{0,E}, \tag{22}$$

$$\|\vec{v}_E b_E\|_{0,T} \leqslant C_k h_E^{1/2} \|\vec{v}_E\|_{0,E}, \tag{23}$$

$$|\vec{v}_E b_E|_{1,T} \leqslant C_k h_E^{-1/2} \|\vec{v}_E\|_{0,E}, \tag{24}$$

where c_k and C_k are two constants which only depend on the element aspect ratio and the polynomial degrees k_0 and k_1.

Here, k_0 and k_1 are fixed and c_k and C_k can be associated with generic constants c and C. In addition, $\vec{v}_E$ which is only defined on the edge E also denotes its natural extension to the element T.

Second, we recall some quasi-interpolation estimates in the following lemma.

Lemma 3.2. *Clément interpolation estimate*: *given $\vec{v} \in \boldsymbol{H}^1$, let $\vec{v}_h \in X^h$ be the quasi-interpolant of $\vec{v}$ defined by averaging as in [7]. For any $T \in T_h$,*

$$\|\vec{v} - \vec{v}_h\|_{0,T} \leqslant C h_T |\vec{v}|_{1,\tilde{\omega}_T}, \tag{25}$$

and for all $E \in \partial T$

$$\|\vec{v} - \vec{v}_h\|_{0,E} \leqslant C h_E^{1/2} |\vec{v}|_{1,\tilde{\omega}_E}. \tag{26}$$

We are now ready to introduce our three alternative error estimators.

3.1. A residual error estimator

The material in this section is well known and can be found in several places, e.g. in Creusé et al. [8], or [10, Section 5.4.2]. The element contribution $\eta_{R,T}$ of the residual error estimator η_R is given by

$$\eta_{R,T}^2 := h_T^2 \|\vec{R}_T\|_{0,T}^2 + \|R_T\|_{0,T}^2 + \sum_{E \in \partial T} h_E \|\vec{R}_E\|_{0,E}^2, \tag{27}$$

and the components in (27) are given by

$$\vec{R}_T := \left\{ \nabla^2 \vec{u}_h - \nabla p_h \right\}\big|_T, \tag{28}$$

$$R_T := \{ \nabla \cdot \vec{u}_h \}|_T, \tag{29}$$

$$\vec{R}_E := \begin{cases} \frac{1}{2} [\![\nabla \vec{u}_h - p_h \mathbf{I}]\!]_E & E \in \varepsilon_{h,\Omega}, \\ -\left(\frac{\partial \vec{u}_h}{\partial \vec{n}_{E,T}} - p_h \vec{n}_{E,T} \right) & E \in \varepsilon_{h,N}, \\ 0 & E \in \varepsilon_{h,D}, \end{cases} \tag{30}$$

with the key contribution coming from the *stress jump* associated with an edge E adjoining elements T and S:

$$[\![\nabla \vec{u}_h - p_h \vec{\mathbf{I}}]\!] := \left((\nabla \vec{u}_h - p_h \vec{\mathbf{I}})|_T - (\nabla \vec{u}_h - p_h \vec{\mathbf{I}})|_S \right) \vec{n}_{E,T}.$$

The *global* residual error estimator is given by $\eta_R := \sqrt{\sum_{T \in T_h} \eta_{R,T}^2}$.

Theorem 3.3. *For any mixed finite element approximation* (*not necessarily inf-sup stable*) *defined on rectangular grids T_h, the residual estimator η_R satisfies*:

$$|\vec{e}|_{1,\Omega} + \|\epsilon\|_{0,\Omega} \leqslant C_\Omega \eta_R,$$

$$\eta_{R,T} \leqslant C \left(\sum_{T' \in \omega_T} \left\{ |\vec{e}|_{1,T'}^2 + \|\epsilon\|_{0,T'}^2 \right\} \right)^{1/2}.$$

Note that the constant C in the local lower bound is independent of the domain.

Proof. We include this for completeness. To establish the upper bound we let $[\vec{v}, q] \in \boldsymbol{H}_{E_0}^1 \times \boldsymbol{P}$ and $\vec{v}_h \in X_h$ be the Clément interpolant of $\vec{v}$, then

$$
\begin{aligned}
\mathfrak{B}\big([\vec{e}, \epsilon]; [\vec{v}, q]\big) &= \mathfrak{B}\big([\vec{e}, \epsilon]; [\vec{v} - \vec{v}_h, q]\big) \\
&= -\big(\nabla \vec{u}_h, \nabla(\vec{v} - \vec{v}_h) \big) + \big(p_h, \nabla \cdot (\vec{v} - \vec{v}_h) \big) + (q, \nabla \cdot u_h) \\
&= \sum_{T \in T_h} \left\{ \big(\nabla^2 \vec{u}_h - \nabla p_h, \vec{v} - \vec{v}_h \big)_T - \sum_{E \in \partial T} \langle \vec{R}_E, \vec{v} - \vec{v}_h \rangle_E + (q, \nabla \cdot \vec{u}_h)_T \right\},
\end{aligned}
$$

where $\langle \vec{R}_E, \vec{v} - \vec{v}_h \rangle_E = \int_E \vec{R}_E \cdot (\vec{v} - \vec{v}_h)$. Thus,

$$\left|\mathfrak{B}\big([\vec{e},\epsilon];[\vec{v},q]\big)\right| \leqslant \sum_{T\in T_h}\left\{\|\nabla^2\vec{u}_h-\nabla p_h\|_{0,T}\|\vec{v}-\vec{v}_h\|_{0,T}+\sum_{E\in\partial T}\|\vec{R}_E\|_{0,E}\|\vec{v}-\vec{v}_h\|_{0,E}+\|q\|_{0,T}\|\nabla\cdot\vec{u}_h\|_{0,T}\right\}$$

$$\leqslant C\Bigg\{\bigg(\sum_{T\in T_h}h_T^2\|\nabla^2\vec{u}_h-\nabla p_h\|_{0,T}^2\bigg)^{1/2}\bigg(\sum_{T\in T_h}\frac{1}{h_T^2}\|\vec{v}-\vec{v}_h\|_{0,T}^2\bigg)^{1/2}$$

$$+\bigg(\sum_{T\in T_h}\sum_{E\in\partial T}h_E\|\vec{R}_E\|_{0,T}^2\bigg)^{1/2}\bigg(\sum_{T\in T_h}\sum_{E\in\partial T}\frac{1}{h_E}\|\vec{v}-\vec{v}_h\|_{0,E}^2\bigg)^{1/2}$$

$$+\bigg(\sum_{T\in T_h}\|q\|_{0,T}^2\bigg)^{1/2}\bigg(\sum_{T\in T_h}\|\nabla\cdot\vec{u}_h\|_{0,T}^2\bigg)^{1/2}\Bigg\}.$$

Using Lemma 3.2 then gives

$$\left|\mathfrak{B}\big([\vec{e},\epsilon];[\vec{v},q]\big)\right| \leqslant C\bigg(\sum_{T\in T_h}\big\{|\vec{v}|_{1,T}^2+\|q\|_{0,T}\big\}\bigg)^{1/2}\bigg(\sum_{T\in T_h}\Big\{h_T^2\|\vec{R}_T\|_{0,T}+\sum_{E\in\partial T}h_E\|\vec{R}_E\|_{0,E}^2+\|R_T\|_{0,T}^2\Big\}\bigg)^{1/2}.$$

Finally, noting that $\vec{e}=\vec{u}-\vec{u}_h\in\boldsymbol{H}_{E_0}^1$ and using (9) gives

$$|\vec{e}|_{1,\Omega}+\|\epsilon\|_{0,\Omega}\leqslant C_\Omega\bigg(\sum_{T\in T_h}\Big\{h_T^2\|\vec{R}_T\|_{0,T}+\sum_{E\in\partial T}h_E\|\vec{R}_E\|_{0,E}^2+\|R_T\|_{0,T}^2\Big\}\bigg)^{1/2}.$$

This establishes the upper bound.

Turning to the local lower bound. First, for the element interior residual part, we set $\vec{w}_T:=\vec{R}_T b_T$. Since $\vec{w}_T=0$ on ∂T, it can be extended to the whole of Ω by setting $\vec{w}_T=0$ in $\Omega\setminus T$ to give an extended function that is in $\boldsymbol{H}_{E_0}^1$. Then,

$$(\nabla\vec{u}-p\mathrm{I},\nabla\vec{w}_T)_T=(\nabla\vec{u}-p\mathrm{I},\nabla\vec{w}_T)_\Omega=0. \tag{31}$$

With (31),

$$\begin{aligned}
(\vec{R}_T,\vec{w}_T)_T &= \big(\nabla^2\vec{u}_h-\nabla p_h,\vec{w}_T\big)_T\\
&= -(\nabla\vec{u}_h-p_h\mathrm{I},\nabla\vec{w}_T)_T+\big\langle(\nabla\vec{u}_h-p_h\mathrm{I})\cdot\vec{n},\vec{w}_T\big\rangle_{\partial T}\\
&= -(\nabla\vec{u}_h-p_h\mathrm{I},\nabla\vec{w}_T)_T\\
&= -(\nabla\vec{u}_h-p_h\mathrm{I},\nabla\vec{w}_T)_T+(\nabla\vec{u}-p\mathrm{I},\nabla\vec{w}_T)_T\\
&= (\nabla\vec{e}-\epsilon\mathrm{I},\nabla\vec{w}_T)_T\\
&\leqslant \big(|\vec{e}|_{1,T}+\|\epsilon\|_{0,T}\big)|\vec{w}_T|_{1,T}\\
&\leqslant \big(|\vec{e}|_{1,T}^2+\|\epsilon\|_{0,T}^2\big)^{1/2}h_T^{-1}\|\vec{R}_T\|_{0,T},
\end{aligned} \tag{32}$$

where in (32), $\langle(\nabla\vec{u}_h-p_h\mathrm{I})\vec{n},\vec{w}_E\rangle_{\partial T}=\int_{\partial T}(\nabla\vec{u}_h-p_h\mathrm{I})\vec{n}\cdot\vec{w}_E$. In addition, from the inverse inequality (20), $(\vec{R}_T,\vec{w}_T)_T=\|\vec{R}_T b_T^{1/2}\|_{0,T}^2\geqslant c\|\vec{R}_T\|_{0,T}^2$, thus

$$h_T^2\|\vec{R}_T\|_{0,T}^2\leqslant C\big(|\vec{e}|_{1,T}^2+\|\epsilon\|_{0,T}^2\big). \tag{33}$$

Next comes the divergence part,

$$\|R_T\|_{0,T}=\|\nabla\cdot\vec{u}_h\|_{0,T}=\big\|\nabla\cdot(\vec{u}-\vec{u}_h)\big\|_{0,T}\leqslant\sqrt{2}|\vec{u}-\vec{u}_h|_{1,T}=\sqrt{2}|\vec{e}|_{1,T}. \tag{34}$$

Finally, we need to estimate the jump term. For an edge $E\in\partial T\cap\varepsilon_{h,\Omega}$ we set $\vec{w}_E=\vec{R}_E b_E$ so that

$$2\langle\vec{R}_E,\vec{w}_E\rangle_E=\sum_{i=1:2}\big\langle(\nabla\vec{u}_h-p_h\mathrm{I})\vec{n},\vec{w}_E\big\rangle_{\partial T}=(\nabla\vec{u}_h-p_h\mathrm{I},\nabla\vec{w}_E)_{\omega_E}+\sum_{i=1:2}\big(\nabla^2\vec{u}_h-\nabla p_h,\vec{w}_E\big)_{T_i}.$$

Using the same argument as for (31), the following equality holds,

$$(\nabla\vec{u}-p\mathrm{I},\nabla\vec{w}_E)_{\omega_E}=0, \tag{35}$$

and then, using inverse inequalities gives

$$2\langle \vec{R}_E, \vec{w}_E \rangle_E = -(\nabla \vec{e} - \epsilon I, \nabla \vec{w}_E)_{\omega_E} + \sum_{i=1:2} (\nabla^2 \vec{u}_h - \nabla p_h, \vec{w}_E)_{T_i}$$

$$\leqslant (|\vec{e}|_{1,\omega_E} + \|\epsilon\|_{0,\omega_E})|\vec{w}_E|_{1,\omega_E} + \sum_{i=1:2} \|\vec{R}_{T_i}\|_{0,T_i} \|\vec{w}_E\|_{0,\omega_E}$$

$$\leqslant C\left((|\vec{e}|_{1,\omega_E} + \|\epsilon\|_{0,\omega_E})h_E^{-1/2}\|\vec{R}_E\|_{0,E} + \sum_{i=1:2} \|\vec{R}_{T_i}\|_{0,T_i} h_E^{1/2} \|\vec{R}_E\|_E \right)$$

$$\leqslant C\left((|\vec{e}|_{1,\omega_E}^2 + \|\epsilon\|_{0,\omega_E}^2)^{1/2}h_E^{-1/2}\|\vec{R}_E\|_{0,E} + \sum_{i=1:2} \|\vec{R}_{T_i}\|_{0,T_i} h_E^{1/2} \|\vec{R}_E\|_E \right).$$

Using (33) gives

$$2\langle \vec{R}_E, \vec{w}_E \rangle_E \leqslant C(|\vec{e}|_{1,\omega_E}^2 + \|\epsilon\|_{0,\omega_E}^2)^{1/2}h_E^{-1/2}\|\vec{R}_E\|_{0,E}. \tag{36}$$

Using (22) gives $\langle \vec{R}_E, \vec{w}_E \rangle_E = \|\vec{R}_E b_E^{1/2}\|_{0,E}^2 \geqslant c\|\vec{R}_E\|_{0,E}^2$, and thus using (36) gives

$$h_E\|\vec{R}_E\|_{0,E}^2 \leqslant C(|\vec{e}|_{1,\omega_E}^2 + \|\epsilon\|_{0,\omega_E}^2). \tag{37}$$

We also need to show that (37) holds for boundary edges. First, for the Dirichlet boundary edges, the flux jump is set to be zero, thus (37) trivially holds. Second, for an edge $En \in \partial T \cap \varepsilon_{h,N}$, we again set $\vec{w} = \vec{R}_{En}b_{En}$,

$$\langle \vec{R}_{En}, \vec{w}_{En} \rangle_{En} = \langle (\nabla \vec{u}_h - p_h I)\vec{n}, \vec{w}_{En} \rangle_{\partial T} = (\nabla \vec{u}_h - p_h I, \nabla \vec{w}_{En})_T + (\nabla^2 \vec{u}_h - \nabla p_h, \vec{w}_{En})_T.$$

Thus, as for (35), we have that

$$(\nabla \vec{u} - pI, \nabla \vec{w}_{En})_T = 0.$$

Then, using the inverse inequalities and following the argument above gives

$$h_{En}\|\vec{R}_{En}\|_{0,En}^2 \leqslant C(|\vec{e}|_{1,T}^2 + \|\epsilon\|_{0,T}^2). \tag{38}$$

Finally, combining (33), (34), (37) and (38) establishes the local lower bound. $\quad\square$

Remark 3.4. Theorem 3.3 also holds for stable (and unstable) mixed approximations defined on a triangular subdivision. The proof is essentially identical to the rectangular case. Specifically, the upper bound can be established directly using the Clément interpolation for triangular meshes. In order to show the local lower bound, we just need to repeat the process for rectangular meshes using a cubic *element* bubble function defined by taking the value one at the centroid of the triangle and zero on the three edges, together with an *edge* bubble function defined by a quadratic polynomial which takes value one at the midpoint of one edge and is zero on the other two edges.

3.2. A local Stokes problem error estimator

Here our focus is on the $\mathbf{Q}_2$–$\mathbf{P}_{-1}$ approximation method. Specifically, a suitable correction space $\mathbf{Q}_T$ needs to be introduced at this point. For an interior rectangle (i.e. if all four edges are in $\varepsilon_{h,\Omega} \cup \varepsilon_{h,N}$), $\mathbf{Q}_T$ is the $(\mathbf{Q}_3(T))^2$ space excluding the basis functions associated with the four vertices, and for an element with some edges in $\varepsilon_{h,D}$, $\mathbf{Q}_T$ is the $(\mathbf{Q}_3(T))^2$ space excluding the basis functions associated with the four vertices and all the other nodes on the boundary $\partial \Omega_D$. For a rectangle containing edges in $\varepsilon_{h,D}$, it is assumed that at most two neighboring edges are in $\varepsilon_{h,D}$. If the rectangle T has only one edge in $\varepsilon_{h,D}$, we call it an *edge* element, whereas if it has two neighboring edges in $\varepsilon_{h,D}$, we call it a *corner* element. Fig. 2 illustrates the types of correction spaces that can arise.

The local Stokes problem estimator $\eta_S = \sqrt{\sum_{T \in T_h} \eta_{S,T}^2}$ is then defined as follows,

$$\eta_{S,T}^2 = |\vec{e}_{S,T}|_{1,T}^2 + \|\epsilon_{S,T}\|_{0,T}^2, \tag{39}$$

where $(\vec{e}_{S,T}, \epsilon_{S,T}) \in \mathbf{Q}_T \times \mathbf{Q}_2(T)$ satisfies

$$(\nabla \vec{e}_{S,T}, \nabla \vec{v})_T - (\epsilon_{S,T}, \nabla \cdot \vec{v})_T = (\vec{R}_T, \vec{v})_T - \sum_{E \in \partial T} \langle \vec{R}_E, \vec{v} \rangle_E \quad \forall \vec{v} \in \mathbf{Q}_T, \tag{40}$$

$$(\nabla \cdot \vec{e}_{S,T}, q) = (R_T, q)_T \quad \forall q \in \mathbf{Q}_2(T). \tag{41}$$

Note that (40)–(41) represents a Stokes problem posed on an element T with a Neumann (zero flux) boundary condition. Although the velocity solution for a Stokes problem is not uniquely defined when a zero flux condition applies everywhere on the boundary, the special choice of correction space $\mathbf{Q}_T$ guarantees that the system (40)–(41) always has a unique solution.
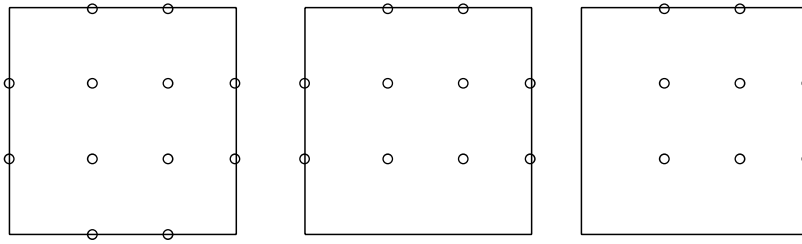
Fig. 2. The correction space $\mathbf{Q}_T$ for an interior element (left), for an edge element (middle) and for a corner element (right).

We want to establish that the Stokes estimator $\eta_{S,T}$ is equivalent to the residual estimator $\eta_{R,T}$. The following local inf-sup stability estimate will be crucial in achieving this goal.

Lemma 3.5. *Local inf-sup stability*: *for* $\mathbf{Q}_2$–$\mathbf{P}_{-1}$ *approximation on any rectangle* $T \in T_h$, *there exists a positive constant* γ_L *independent of h, such that*

$$\min_{0 \neq q_h \in \mathbf{Q}_2(T)} \max_{\vec{0} \neq \vec{v}_h \in \mathbf{Q}_T} \frac{|(q_h, \nabla \cdot \vec{v}_h)|}{|\vec{v}_h|_1 \|q_h\|_0} \geq \gamma_L. \tag{42}$$

Proof. Our proof is a generalization of the approach of Verfürth [17, Lemma 4.1]. First, for the reference element $\tilde{T}$, the local inf-sup stability associated with the three types of $\mathbf{Q}_T$ can be established by direct computation of the minimum eigenvalue in (15). Next, for an arbitrary element T, we let F_T denote the affine map from $\tilde{T}$ to T and denote the Jacobian determinant of F_T by $|J| = h_{T,x}h_{T,y}$, where $h_{T,x}$ and $h_{T,y}$ are the element sizes in x and y directions respectively. Thus, for any $q \in \mathbf{Q}_2(T)$, we define $q_\star := |J|^{1/2} q \circ F_T \in \mathbf{Q}_2(\tilde{T})$. Then, there exists a $\vec{u}_\star = (u_{x,\star}, u_{y,\star})^T \in \mathbf{Q}_{\tilde{T}}$ with $|\vec{u}_\star|_{1,\tilde{T}} = \|q_\star\|_{0,\tilde{T}}$, such that

$$(\nabla \cdot \vec{u}_\star, q_\star)_{\tilde{T}} \geq \tilde{\gamma} \|q_\star\|_{0,\tilde{T}}^2 \tag{43}$$

where $\tilde{\gamma}$ is the local inf-sup constant for the reference element $\tilde{T}$. If we further define

$$\vec{u}_T := \begin{pmatrix} |J|^{1/2} \frac{1}{h_{T,y}} u_{x,\star} \circ F_T^{-1} \\ |J|^{1/2} \frac{1}{h_{T,x}} u_{y,\star} \circ F_T^{-1} \end{pmatrix}, \tag{44}$$

then, using (s, t) to denote the local coordinates for the reference element we get

$$|\vec{u}_T|_{1,T}^2 = \int_T \left(\frac{\partial u_{x,T}}{\partial x}\right)^2 + \left(\frac{\partial u_{y,T}}{\partial y}\right)^2$$

$$= \int_{\tilde{T}} \left(\left(|J|^{1/2} \frac{1}{h_{T,y}} \frac{\partial u_{x,\star}}{\partial s} \frac{1}{h_{T,x}}\right)^2 + \left(|J|^{1/2} \frac{1}{h_{T,x}} \frac{\partial u_{y,\star}}{\partial t} \frac{1}{h_{T,y}}\right)^2\right) |J|$$

$$= |\vec{u}_\star|_{1,\tilde{T}}^2 = \|q_\star\|_{0,\tilde{T}}^2 = \int_{\tilde{T}} q_\star^2 = \int_T \left(|J|^{1/2} q_T\right)^2 |J|^{-1} = \|q_T\|_{0,T}^2.$$

So we see that

$$|\vec{u}_T|_{1,T} = \|q_T\|_{0,T}. \tag{45}$$

Next,

$$(\nabla \cdot \vec{u}_T, q_T)_T = \int_T \frac{\partial u_{x,T}}{\partial x} q_T + \frac{\partial u_{y,T}}{\partial y} q_T$$

$$= \int_{\tilde{T}} \left(|J|^{1/2} \frac{1}{h_{T,y}} \frac{\partial u_{x,\star}}{\partial s} \frac{1}{h_{T,x}} |J|^{-1/2} q_\star + |J|^{1/2} \frac{1}{h_{T,x}} \frac{\partial u_{y,\star}}{\partial t} \frac{1}{h_{T,y}} |J|^{-1/2} q_\star\right) |J|$$

$$= \int_{\tilde{T}} \left(\frac{\partial u_{x,\star}}{\partial s} q_\star + \frac{\partial u_{y,\star}}{\partial t} q_\star\right) = (\nabla \cdot \vec{u}_\star, q_\star)_{\tilde{T}}$$

$$\geq \tilde{\gamma} \|q_\star\|_{0,\tilde{T}}^2 = \tilde{\gamma} \|q_T\|_{0,T}^2. \tag{46}$$

This establishes the stability bound (42) with an inf-sup constant $\gamma_L = \tilde{\gamma}$. □

Mirroring the discussion of the stability of the continuous problem in Section 2 leads us to the following result.

Lemma 3.6. *Local $\mathfrak{B}$-stability*: *if the mixed approximation is locally inf-sup stable, then, for all $(\vec{w}, s) \in \mathbf{Q}_T \times \mathbf{Q}_2(T)$, we have that*

$$\max_{(\vec{v},q)\in\mathbf{Q}_T\times\mathbf{Q}_2(T)} \frac{\mathfrak{B}((\vec{w},s);(\vec{v},q))}{|\vec{v}|_{1,T} + \|q\|_{0,T}} \geqslant \gamma_B \big(|\vec{w}|_{1,T} + \|s\|_{0,T}\big), \tag{47}$$

where γ_B is a positive constant that only depends on the inf-sup constant γ_L in (42).

Proof. See Elman et al. [10, Lemma 5.2]. □

The robustness of the Stokes error estimator is established next.

Theorem 3.7. *For $\mathbf{Q}_2 - \mathbf{P}_{-1}$ approximation on a rectangle $T \in T_h$, the estimator $\eta_{S,T}$ is equivalent to the residual estimator: $c\eta_{S,T} \leqslant \eta_{R,T} \leqslant C\eta_{S,T}$.*

Proof. The proof is a generalization of [14, Theorem 3.5]. The details are sketched out below. First, we need to use (47):

$$\begin{aligned}
\eta_{S,T} &= \sqrt{|\vec{e}_{S,T}|^2_{1,T} + \|\epsilon_{S,T}\|^2_{0,T}} \\
&\leqslant |\vec{e}_{S,T}|_{1,T} + \|\epsilon_{S,T}\|_{0,T} \\
&\leqslant \frac{1}{\gamma_B} \max_{(\vec{v},q)\in\mathbf{Q}_T\times\mathbf{Q}_2(T)} \frac{\mathfrak{B}((\vec{e}_{S,T},\epsilon_{S,T});(\vec{v},q))}{|\vec{v}|_{1,T} + \|q\|_{0,T}} \\
&= \frac{1}{\gamma_B} \max_{(\vec{v},q)\in\mathbf{Q}_T\times\mathbf{Q}_2(T)} \frac{(\vec{R}_T, \vec{v})_T - \sum_{E\in\partial T}\langle \vec{R}_E, \vec{v}\rangle_E - (q, \nabla\cdot\vec{u}_h)_T}{|\vec{v}|_{1,T} + \|q\|_{0,T}} \\
&\leqslant \frac{1}{\gamma_B} \max_{(\vec{v},q)\in\mathbf{Q}_T\times\mathbf{Q}_2(T)} \frac{\|\vec{R}_T\|_{0,T}\|\vec{v}\|_{0,T} + \sum_{E\in\partial T}\|\vec{R}_E\|_{0,E}\|\vec{v}\|_{0,E} + \|q\|_{0,T}\|\nabla\cdot\vec{u}_h\|_{0,T}}{|\vec{v}|_{1,T} + \|q\|_{0,T}}.
\end{aligned} \tag{48}$$

Now, since $\vec{v}$ is zero at the four vertices of T, a scaling argument and the usual trace theorem, see e.g. [10, Lemma 1.5], shows that $\vec{v}$ satisfies

$$\|\vec{v}\|_{0,E} \leqslant Ch_E^{1/2}|\vec{v}|_{1,T}, \tag{49}$$

$$\|\vec{v}\|_{0,T} \leqslant Ch_T|\vec{v}|_{1,T}. \tag{50}$$

Combining these two inequalities with (48) immediately gives the lower bound in the equivalence relation. For the upper bound, we first let $\vec{w}_T = \vec{R}_T b_T$ (b_T is an element interior bubble function). From (40),

$$\begin{aligned}
(\vec{R}_T, \vec{w}_T)_T &= (\nabla\vec{e}_{S,T}, \nabla\vec{w}_T)_T - (\epsilon_{S,T}, \nabla\cdot\vec{w}_T)_T \\
&\leqslant |\vec{e}_{S,T}|_{1,T}|\vec{w}_T|_{1,T} + \|\epsilon_{S,T}\|_{0,T}\|\nabla\cdot\vec{w}_T\|_{0,T} \\
&\leqslant \sqrt{2}|\vec{w}_T|_{1,T}\big(|\vec{e}_{S,T}|_{1,T} + \|\epsilon_{S,T}\|_{0,T}\big) \\
&\leqslant C\frac{1}{h_T}\|\vec{R}_T\|_{0,T}\big(|\vec{e}_{S,T}|^2_{1,T} + \|\epsilon_{S,T}\|^2_{0,T}\big)^{1/2}.
\end{aligned} \tag{51}$$

In addition, from the inverse inequalities, $\|\vec{R}_T\|^2_{0,T} \leqslant C(\vec{R}_T, \vec{w}_T)_T$, and using (51),

$$h_T^2\|\vec{R}_T\|^2_{0,T} \leqslant C\big(|\vec{e}_{S,T}|^2_{1,T} + \|\epsilon_{S,T}\|^2_{0,T}\big). \tag{52}$$

Next, we let $\vec{w}_E = \vec{R}_E b_E$ (b_E is an edge bubble function). Then, from (40) and using (52), (23), together with the estimate $|\vec{w}_E|_{1,T} \leqslant Ch_T^{-1}\|\vec{w}_E\|_{0,T}$, we get

$$\begin{aligned}
\langle\vec{R}_E, \vec{w}_E\rangle_E &= -(\nabla\vec{e}_{S,T}, \nabla\vec{w}_E)_T + (\epsilon_{S,T}, \nabla\cdot\vec{w}_E)_T + (\vec{R}_T, \vec{w}_E)_T \\
&\leqslant |\vec{e}_{S,T}|_{1,T}|\vec{w}_E|_{1,T} + \|\epsilon_{S,T}\|_{0,T}\|\nabla\cdot\vec{w}_E\|_{0,T} + \|\vec{R}_T\|_{0,T}\|\vec{w}_E\|_{0,T} \\
&\leqslant C|\vec{w}_E|_{1,T}\big(|\vec{e}_{S,T}|_{1,T} + \|\epsilon_{S,T}\|_{0,T}\big) + Ch_T^{-1}\big(|\vec{e}_{S,T}|_{1,T} + \|\epsilon_{S,T}\|_{0,T}\big)\|\vec{w}_E\|_{0,T} \\
&\leqslant Ch_T^{-1}\|\vec{w}_E\|_{0,T}\big(|\vec{e}_{S,T}|_{1,T} + \|\epsilon_{S,T}\|_{0,T}\big) \\
&\leqslant Ch_E^{-1/2}\|\vec{R}_E\|_{0,E}\big(|\vec{e}_{S,T}|_{1,T} + \|\epsilon_{S,T}\|_{0,T}\big).
\end{aligned} \tag{53}$$

Then, using $\|\vec{R}_E\|_{0,E}^2 \leqslant C\langle \vec{R}_E, \vec{w}_E \rangle_E$ and (53),

$$h_E \|\vec{R}_E\|_{0,E}^2 \leqslant C\big(|\vec{e}_{S,T}|_{1,T}^2 + \|\epsilon_{S,T}\|_{0,T}^2\big). \tag{54}$$

Finally, from (41), since $\nabla \cdot \vec{u}_h|_T \in \mathbf{Q}_2(T)$ we have that

$$(\nabla \cdot \vec{e}_{S,T}, \nabla \cdot \vec{u}_h)_T = (\nabla \cdot \vec{u}_h, \nabla \cdot \vec{u}_h)_T,$$

$$\|R_T\|_{0,T} = \|\nabla \cdot \vec{u}_h\|_{0,T} \leqslant \|\nabla \cdot \vec{e}_{S,T}\|_{0,T} \leqslant \sqrt{2}|\vec{e}_{S,T}|_{1,T}. \tag{55}$$

Combining (52), (54) and (55), establishes the upper bound in the equivalence relation. □

Remark 3.8. The fact that $\nabla \cdot \vec{u}_h|_T \in \mathbf{Q}_2(T)$ is crucial for the last step above. If we wanted to extend this error estimation approach to other mixed approximations then we would simply need to ensure that the pressure correction space is big enough to contain the divergence of the original velocity space. The only difficulty with this is that we also have to ensure that the velocity correction space is big enough to ensure that the local inf-sup stability condition (42) is not compromised. Thus, if we wanted to develop a Stokes error estimator for the $\mathbf{P}_{2*}$–$\mathbf{P}_{-1}$ mixed approximation, then the first thing to do is to choose a pressure augmentation space that is big enough to contain the divergence of $\mathbf{P}_{2*}$ functions. The standard quadratic polynomial space $\mathbf{P}_2$ would work. We must then choose a velocity augmentation space that is big enough to ensure that the combination of augmented spaces is locally stable. This suggests using a reduced $\mathbf{P}_3$ space for velocities (that is, with the vertex basis functions removed).

The Stokes estimator leads to large dimensional local problems. For example, the dimension of the local Stokes problem that must be solved to estimate the error in the interior element in Fig. 2 is 33×33. Our next approach is much simpler and, as we will see in Section 4, effective in estimating the error in practice.

3.3. A local Poisson problem estimator

The local Poisson problem estimator $\eta_P = \sqrt{\sum_{T \in T_h} \eta_{P,T}^2}$ can be derived from the locally stable Stokes estimator (40)–(41) as follows:

$$\eta_{P,T}^2 = |\vec{e}_{P,T}|_{1,T}^2 + \|\epsilon_{P,T}\|_{0,T}^2, \tag{56}$$

where $(\vec{e}_{P,T}, \epsilon_{P,T}) \in \mathbf{Q}_T \times \mathbf{Q}_2(T)$ satisfies

$$(\nabla \vec{e}_{P,T}, \nabla \vec{v})_T = (\vec{R}_T, \vec{v})_T - \sum_{E \in \partial T} \langle \vec{R}_E, \vec{v} \rangle_E \quad \forall \vec{v} \in \mathbf{Q}_T, \tag{57}$$

$$(\epsilon_{P,T}, q) = (R_T, q)_T \quad \forall q \in \mathbf{Q}_2(T). \tag{58}$$

This is much more appealing from a computational perspective. First, (57) decouples into a pair of local Poisson problems, each one of dimension 12×12 in the case of the interior element in Fig. 2. Second, since by construction $R_T = \nabla \cdot \vec{u}_h \in \mathbf{Q}_2(T)$, the solution of (58) is immediate: $\epsilon_{P,T} = \nabla \cdot \vec{u}_h$. The theoretical justification for computing the Poisson estimator instead of the Stokes estimator is the following equivalence result.

Theorem 3.9. *Given that the spaces defining the Stokes estimator are locally $\mathfrak{B}$-stable, the estimator $\eta_{P,T}$ is equivalent to the Stokes estimator: $c\eta_{S,T} \leqslant \eta_{P,T} \leqslant C\eta_{S,T}$.*

Proof. The proof is a straightforward extension of [14, Thm. 3.6]. We include it here for completeness. Combining (40), (41), (57), (58), for any $T \in T_h$ and $[\vec{v}, q] \in \mathbf{Q}_T \times \mathbf{Q}_2(T)$ we get

$$\begin{aligned}
(\nabla \vec{e}_{P,T}, \nabla \vec{v})_T - (\epsilon_{P,T}, q)_T &= (\vec{R}_T, \vec{v})_T - \sum_{E \in \partial T} \langle \vec{R}_E, \vec{v} \rangle_E - (\nabla \cdot \vec{u}_h, q)_T \\
&= (\nabla \vec{e}_{S,T}, \nabla \vec{v})_T - (\epsilon_{S,T}, \nabla \cdot \vec{v})_T - (\nabla \cdot \vec{e}_{S,T}, q)_T \\
&= \mathfrak{B}\big((\vec{e}_{S,T}, \epsilon_{S,T}); (\vec{v}, q)\big).
\end{aligned} \tag{59}$$

Then, using the local $\mathfrak{B}$-stability (47) gives

$$\begin{aligned}
|\vec{e}_{S,T}|_{1,T} + \|\epsilon_{S,T}\|_{0,T} &\leqslant \frac{1}{\gamma_B} \max_{(\vec{v},q) \in \mathbf{Q}_T \times \mathbf{Q}_2(T)} \frac{\mathfrak{B}((\vec{e}_{S,T}, \epsilon_{S,T}); (\vec{v}, q))}{|\vec{v}|_{1,T} + \|q\|_{0,T}} \\
&= \frac{1}{\gamma_B} \max_{(\vec{v},q) \in \mathbf{Q}_T \times \mathbf{Q}_2(T)} \frac{(\nabla \vec{e}_{P,T}, \nabla \vec{v})_T - (\epsilon_{P,T}, q)_T}{|\vec{v}|_{1,T} + \|q\|_{0,T}}
\end{aligned}$$

$$\leqslant \frac{1}{\gamma_B} \max_{(\vec{v},q)\in\mathbf{Q}_T\times\mathbf{Q}_2(T)} \frac{|\vec{e}_{P,T}|_{1,T}|\vec{v}|_{1,T} + \|\epsilon_{P,T}\|_{0,T}\|q\|_{0,T}}{|\vec{v}|_{1,T} + \|q\|_{0,T}}$$

$$\leqslant \frac{1}{\gamma_B}\big(|\vec{e}_{P,T}|_{1,T} + \|\epsilon_{P,T}\|_{0,T}\big). \tag{60}$$

This establishes the lower bound in the equivalence relation. In order to show the upper bound, we take $\vec{v} \in \mathbf{Q}_T$, and then using (40) and (57) we get

$$(\nabla \vec{e}_{P,T}, \nabla \vec{v})_T = (\vec{R}_T, \vec{v})_T - \sum_{E\in\partial T}\langle \vec{R}_E, \vec{v}\rangle_E$$

$$= (\nabla \vec{e}_{S,T}, \nabla \vec{v})_T - (\epsilon_{S,T}, \nabla \cdot \vec{v})_T. \tag{61}$$

Using (41) and (58) means that, for any $q \in \mathbf{Q}_2(T)$,

$$(\epsilon_{P,T}, q)_T = (R_T, q)_T = (\nabla \cdot \vec{e}_{S,T}, q). \tag{62}$$

Using (61) gives

$$|\vec{e}_{P,T}|_{1,T} = \max_{\vec{v}\in\mathbf{Q}_T} \frac{(\nabla \vec{e}_{P,T}, \nabla \vec{v})_T}{|\vec{v}|_{1,T}} = \max_{\vec{v}\in\mathbf{Q}_T} \frac{(\nabla \vec{e}_{S,T}, \nabla \vec{v})_T - (\epsilon_{S,T}, \nabla \cdot \vec{v})_T}{|\vec{v}|_{1,T}}$$

$$\leqslant \max_{\vec{v}\in\mathbf{Q}_T} \frac{|\vec{e}_{S,T}|_{1,T}|\vec{v}|_{1,T} + \|\epsilon_{S,T}\|_{0,T}\|\nabla \cdot \vec{v}\|_{0,T}}{|\vec{v}|_{1,T}} \leqslant |\vec{e}_{S,T}|_{1,T} + \sqrt{2}\|\epsilon_{S,T}\|_{0,T}, \tag{63}$$

and, using (62),

$$\|\epsilon_{P,T}\|_{0,T} = \max_{q\in\mathbf{Q}_2(T)} \frac{(\epsilon_{P,T}, q)_T}{\|q\|_{0,T}} = \max_{q\in\mathbf{Q}_2(T)} \frac{(\nabla \cdot \vec{e}_{S,T}, q)_T}{\|q\|_{0,T}}$$

$$\leqslant \max_{q\in\mathbf{Q}_2(T)} \frac{\|\nabla \cdot \vec{e}_{S,T}\|_{0,T}\|q\|_{0,T}}{\|q\|_{0,T}} = \|\nabla \cdot \vec{e}_{S,T}\| \leqslant \sqrt{2}|\vec{e}_{S,T}|_{1,T}. \tag{64}$$

Finally, combining (63) with (64) gives the required upper bound. $\square$

Remark 3.10. If we wanted to extend this error estimation approach to other mixed approximations then we simply need to ensure that the pressure correction space is big enough to contain the divergence of the original velocity space. The upshot of this is that the Poisson estimator is independent of the pressure approximation—we would also solve (57)–(58) if we wanted to estimate the error in a solution computed with $\mathbf{Q}_2$–$\mathbf{Q}_1$ or $\mathbf{Q}_2$–$\mathbf{P}_0$ approximation!

4. Computational experiments

In this section two test problems are solved in order to compare the effectivity of three error estimation strategies: a modified residual estimator $\tilde{\eta}_R$, and the Poisson estimator η_P as implemented in the IFISS Matlab toolbox [15]; and a local recovery Z–Z estimator η_Z as implemented in the Oomph-lib package [12]. The modified residual error estimator was introduced by Paul Houston et al. [13], and is defined as follows:

$$\tilde{\eta}_{R,T}^2 := \left(\frac{h_T}{2}\right)^2 \|\vec{R}_T\|_{0,T}^2 + \|R_T\|_{0,T}^2 + \sum_{E\in\partial T}\frac{h_E}{2}\|\vec{R}_E\|_{0,E}^2, \tag{65}$$

and $\tilde{\eta}_R := \sqrt{\sum_{T\in\mathcal{T}_h}\tilde{\eta}_{R,T}^2}$. We focus on this modified residual estimator $\tilde{\eta}_R$ because our computational experience shows that $\tilde{\eta}_R$ is much more accurate than the standard residual estimator η_R. The Z–Z estimator is a popular error estimation strategy: it is also considered by practitioners to be one the best in terms of its simplicity and reliability, especially when used as a refinement indicator in a self-adaptive refinement setting.

4.1. Test problem 1: A smooth solution

Our first test problem is hard-wired into the IFISS package [9, problem S4], and the solution is a quartic polynomial:

$$\vec{u} = \begin{pmatrix} 20xy^3 \\ 5x^4 - 5y^4 \end{pmatrix}, \quad p = 60x^2y - 20y^3. \tag{66}$$

We solve the problem as an enclosed flow (that is $\partial\Omega_N = \emptyset$) with the boundary data $\vec{w}$ given by interpolating the exact flow solution at the nodes. We could account for the resulting "variational crime" by using the methodology introduced

Table 1
Comparison of error estimator effectivity.

h	e	$\frac{e}{\tilde{\eta}_R}$	$\frac{e}{\eta_P}$	$\frac{e}{\eta_Z}$
$\frac{1}{4}$	1.0278e+00	5.1508e−01	1.0909e+00	3.7098e+00
$\frac{1}{8}$	2.5569e−01	4.9210e−01	1.0189e+00	3.2837e+00
$\frac{1}{16}$	6.3825e−02	4.8148e−01	9.8762e−01	3.0741e+00
$\frac{1}{32}$	1.5950e−02	4.7638e−01	9.7317e−01	2.9737e+00

(a) Exact error: e_T

(b) Estimator: $\tilde{\eta}_{R,T}$

(c) Estimator: $\eta_{P,T}$

(d) Estimator: $\eta_{Z,T}$
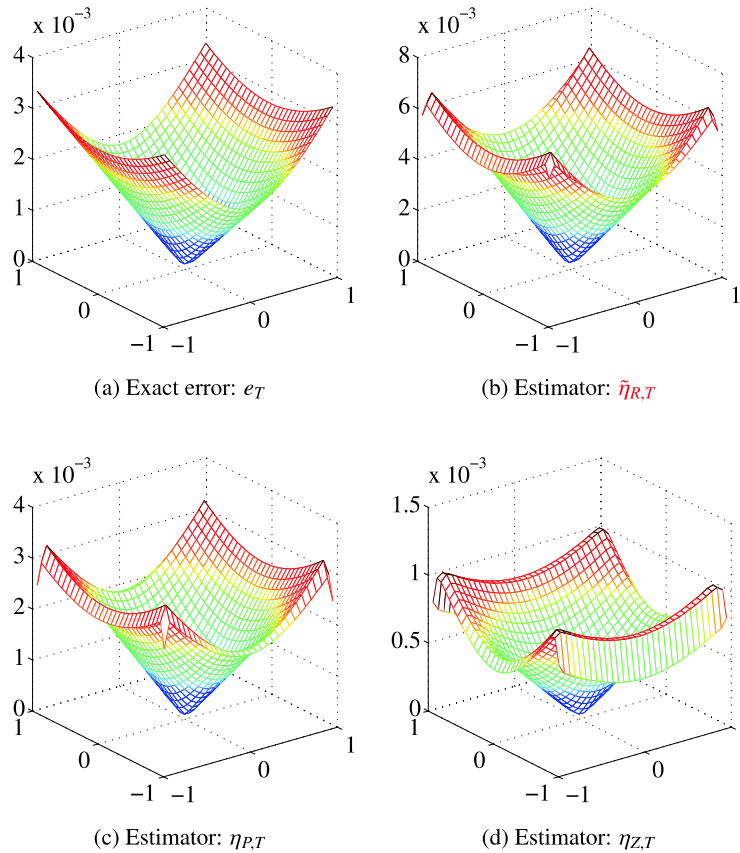
Fig. 3. The exact error and estimated errors for test problem 1 with $h = \frac{1}{16}$.

by Ainsworth and Kelly [1], but have not done so in the results reported below.[1] The flow problem is solved on a square domain $(-1, 1) \times (-1, 1)$ using a nested sequence of uniformly refined square grids. The coarsest grid is 8×8 and is associated with a mesh parameter of $h = 1/4$. To interpret the results that are presented some notation will be needed:

$$e = \sqrt{|\vec{u} - \vec{u}_h|_1^2 + \|p - p_h\|_0^2}, \tag{67}$$

$$e_T = \sqrt{|\vec{u} - \vec{u}_h|_{1,T}^2 + \|p - p_h\|_{0,T}^2}, \tag{68}$$

while e_{ω_T} is defined analogously to e_T. Looking first at Table 1, we see that the global error e is decreasing like $O(h^2)$ as expected. It is also evident that the Poisson problem estimator η_P provides the most accurate estimate of the global error: $\frac{e}{\eta_P}$ is close to one, whereas $\tilde{\eta}_R$ is about twice of the exact error and η_Z is about three times smaller than the exact error. Turning to Fig. 3 we see that all three error estimators seem to be able to correctly indicate the structure of the error, although the vertical scale may not be very accurate. As might be anticipated from the results in Table 1, the only estimator that is quantitatively close to the exact error is $\eta_{P,T}$.

---

[1] This means that the error estimation is inaccurate for elements next to the boundary. These effects are evident in the estimated error plots in Fig. 3.
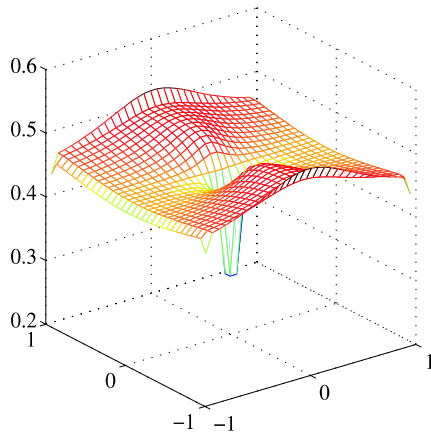
Table 2
Comparison of effectivity indices.

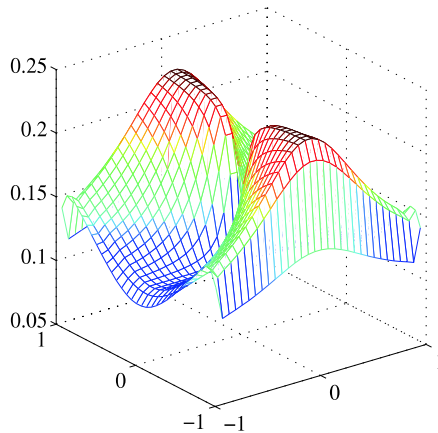| h	e	$\max_{T \in T_h} \frac{e_T}{e_{\omega_T}}$	$\max_{T \in T_h} \frac{\tilde{\eta}_{R,T}}{e_{\omega_T}}$	$\max_{T \in T_h} \frac{\eta_{P,T}}{e_{\omega_T}}$	$\max_{T \in T_h} \frac{\eta_{Z,T}}{e_{\omega_T}}$
$\frac{1}{4}$	1.0278e+00	6.3048e−01	1.1261e+00	5.2173e−01	1.9083e−01
$\frac{1}{8}$	2.5569e−01	6.0283e−01	1.1401e+00	5.2674e−01	2.2408e−01
$\frac{1}{16}$	6.3825e−02	5.8974e−01	1.1327e+00	5.2173e−01	2.3030e−01
$\frac{1}{32}$	1.5950e−02	5.8346e−01	1.1261e+00	5.1777e−01	2.3134e−01
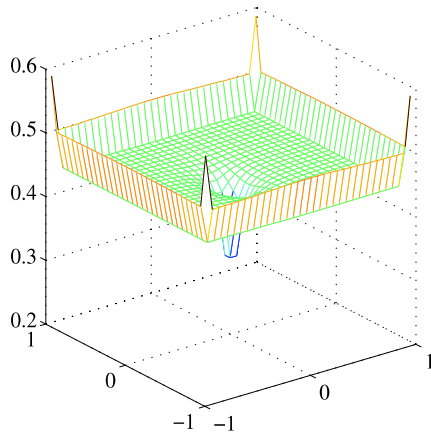
(a) Exact effectivity: $\frac{e_T}{e_{\omega_T}}$
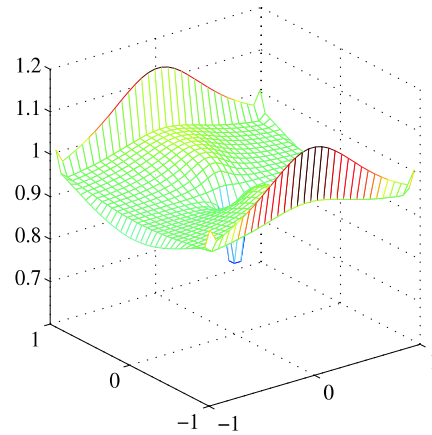
(b) Estimator effectivity: $\frac{\tilde{\eta}_{R,T}}{e_{\omega_T}}$

(c) Estimator effectivity: $\frac{\eta_{P,T}}{e_{\omega_T}}$

(d) Estimator effectivity: $\frac{\eta_{Z,T}}{e_{\omega_T}}$

Fig. 4. The local effectivities of the exact error and the error estimators for test problem 1 with $h = \frac{1}{16}$.

It is instructive to look at the local error estimates in more detail. In general, if an error estimator is to be efficient then the constant on the right-hand side of (18) should be bounded. An estimate of this constant (e.g. $\max_{T \in T_h} \frac{\tilde{\eta}_{R,T}}{e_{\omega_T}}$ for $\tilde{\eta}_R$) is provided in Table 2, where we also estimate this constant for the exact error ($\max_{T \in T_h} \frac{e_T}{e_{\omega_T}}$) and refer to it as the "exact value". From the table, although $\max_{T \in T_h} \frac{\tilde{\eta}_{R,T}}{e_{\omega_T}}$, $\max_{T \in T_h} \frac{\eta_{P,T}}{e_{\omega_T}}$ and $\max_{T \in T_h} \frac{\eta_{Z,T}}{e_{\omega_T}}$ all appear to be bounded, only $\max_{T \in T_h} \frac{\eta_{P,T}}{e_{\omega_T}}$ is close to the "exact value".

Ideally, the local effectivity indices (i.e. $\frac{\tilde{\eta}_{R,T}}{e_{\omega_T}}$ for $\tilde{\eta}_R$) will be bounded above and below across the whole domain, so that elements with large errors can be singled out for local mesh refinement. This is assessed in Fig. 4. Looking at the distribution of these indices it is clear that $\eta_{P,T}$ and $\tilde{\eta}_{R,T}$ are closely aligned with the exact error but the Z–Z estimator is not. In particular the Z–Z estimator has relatively large local effectivity indices in the "wrong place", which could lead to the labelling of elements with small error for adaptive refinement.
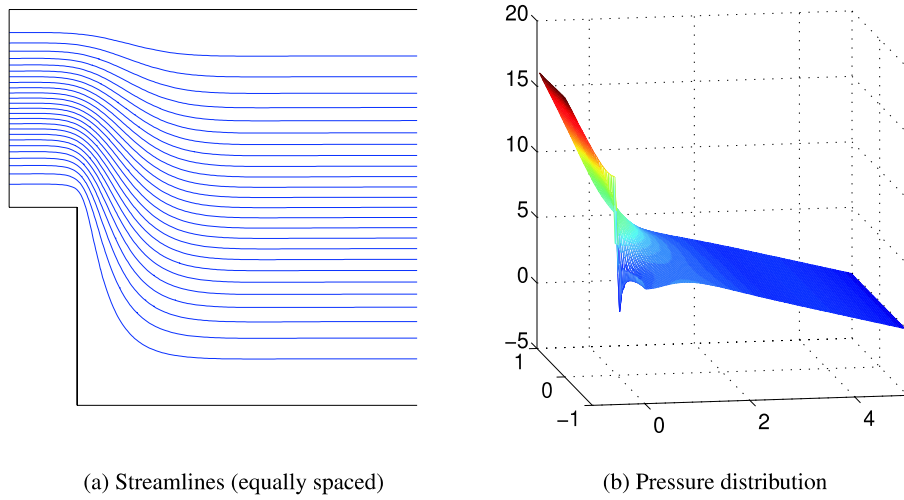
(a) Streamlines (equally spaced)

(b) Pressure distribution

Fig. 5. The Q_2–P_1 solution to test problem 2 with $h = \frac{1}{16}$.

(a) Estimator: $\tilde{\eta}_{R,T}$

(b) Estimator: $\eta_{P,T}$
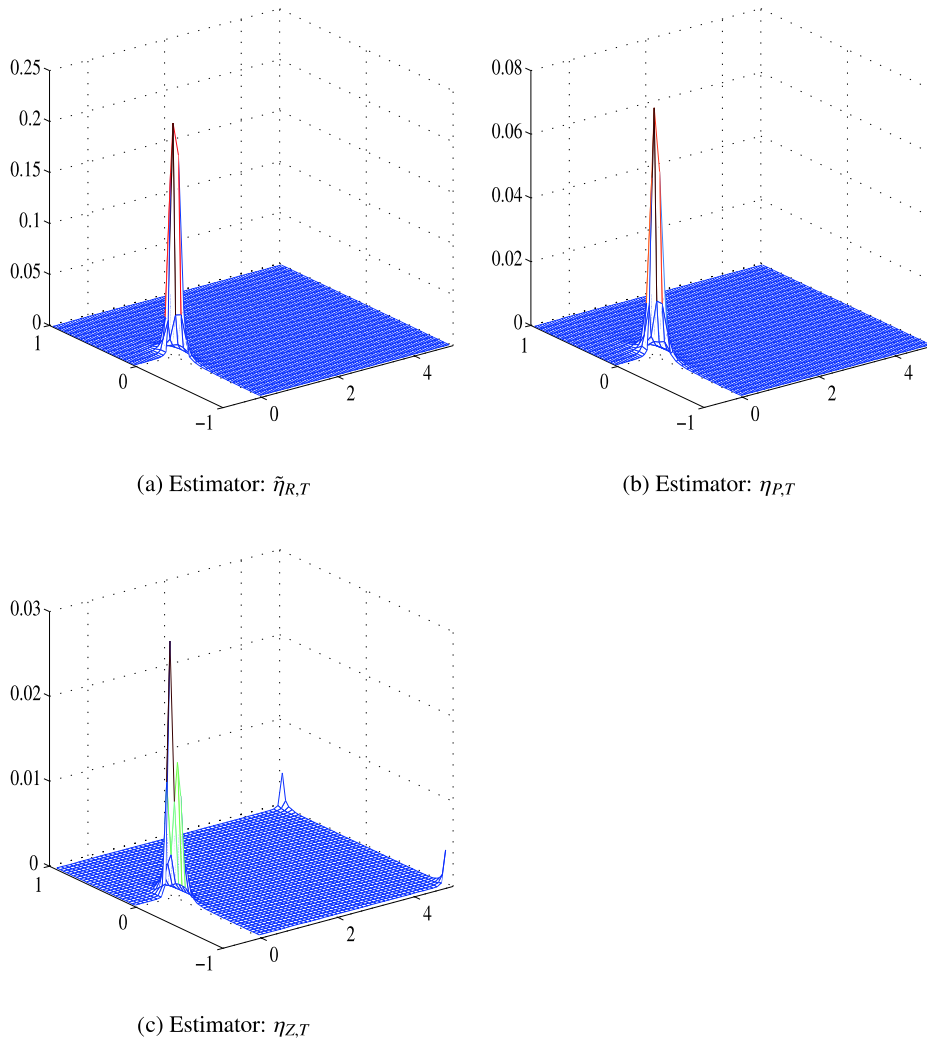

(c) Estimator: $\eta_{Z,T}$

Fig. 6. Estimated distribution of errors for test problem 2 with $h = \frac{1}{16}$.

4.2. Test problem 2: Channel flow over a backward step

The second example is also hard-wired into the IFISS package [9, problem S2]. The flow domain is $(-1, 5) \times (-1, 1) \setminus (-1, 0] \times (-1, 0]$. A zero velocity condition applied at the top and bottom of the channel and fully developed parabolic velocity profile is specified at the inflow boundary ($x = -1$). A natural boundary condition applies at the outflow ($x = 5$). Unlike the first problem, which has a perfectly smooth solution, this problem has a singularity at the re-entrant corner. We solve it using $\boldsymbol{Q}_2$–$\boldsymbol{P}_1$ approximation with a uniform square mesh (with $h = \frac{1}{16}$). The computed solution is shown in Fig. 5 and the profiles of the estimated error using our three estimators are shown in Fig. 6. All three have essentially the same structure—the estimated errors are dominated by the results in the elements close to the singularity. Their magnitudes are different however: the residual estimator is the largest, the Z–Z estimator is the smallest, and the local Poisson estimator is in the middle. This is consistent with the results obtained for the first test problem.

5. Conclusion

Our main conclusion is that the solution of local Poisson problems provides a cheap and effective way of estimating the local discretisation error when solving practical flow problems. Our numerical results make it clear that a global upper bound and a local lower bound on the approximation error do not automatically lead to an effective error estimator in an adaptive refinement setting. Although there is a theoretical guarantee that elements with large errors will be flagged by such an estimator, there is no guarantee that elements that are flagged as having a small discretization error actually have a small error in reality.

References

[1] M. Ainsworth, D.W. Kelly, A posteriori error estimators and adaptivity for finite element approximation of the non-homogeneous Dirichlet problem, Adv. Comput. Math. 15 (2001) 3–23.
[2] M. Ainsworth, J. Oden, A posteriori error estimates for Stokes' and Oseen's equations, SIAM J. Numer. Anal. 34 (1997) 228–245.
[3] M. Ainsworth, J. Oden, A Posteriori Error Estimation in Finite Element Analysis, Wiley, New York, 2000.
[4] R.E. Bank, B. Welfert, A posteriori error estimates for the Stokes problem, SIAM J. Numer. Anal. 28 (1991) 591–623.
[5] D. Braess, Finite Elements, Cambridge University Press, London, 1997.
[6] E. Chizhonkov, M. Olshanskii, On the domain geometry dependence of the LBB condition, M2AN 34 (2000) 935–951.
[7] P. Clément, Approximation by finite element functions using local regularization, R.A.I.R.O. Anal. Numér. 2 (1975) 77–84.
[8] E. Creusé, G. Kunert, S. Nicaise, A posteriori error estimation for the Stokes problem: Anisotropic and isotropic discretizations, M3AS 14 (2004) 1297–1341.
[9] H. Elman, A. Ramage, D. Silvester, Algorithm 866: IFISS, a Matlab toolbox for modelling incompressible flow, ACM Trans. Math. Soft. 33 (2007) 2–14.
[10] H. Elman, D. Silvester, A. Wathen, Finite Elements and Fast Iterative Solvers: With Applications in Incompressible Fluid Dynamics, Oxford University Press, Oxford, ISBN 978-0-19-852868-5, 2005, xiv+400 pp., ISBN 0-19-852868-X.
[11] V. Girault, P.-A. Raviart, Finite Element Methods for Navier–Stokes Equations, Springer-Verlag, Berlin, 1986.
[12] M. Heil, A.L. Hazel, Oomph-lib—an object-oriented multi-physics finite-element library, in: Lect. Notes Comput. Sci. Eng., vol. 53, Springer, 2006, pp. 19–49.
[13] P. Houston, D. Schötzau, T.P. Wihler, hp-adaptive discontinuous Galerkin finite element methods for the Stokes problem, in: P. Neittaanmäki, T. Rossi, S. Korotov, E. Oñate, J. Périaux, D. Knörzer (Eds.), Proceedings of the European Congress on Computational Methods in Applied Sciences and Engineering, vol. II, 2004.
[14] D. Kay, D. Silvester, A posteriori error estimation for stabilized mixed approximations of the Stokes equations, SIAM J. Sci. Comput. 21 (1999) 1321–1336.
[15] D. Silvester, H. Elman, A. Ramage, Incompressible Flow and Iterative Solver Software (IFISS) version 3.0, http://www.manchester.ac.uk/ifiss.
[16] R. Stenberg, Analysis of mixed finite element methods for the Stokes problem: A unified approach, Math. Comp. 42 (1984) 9–23.
[17] R. Verfürth, A posteriori error estimators for the Stokes equations, Numer. Math. 55 (1989) 309–325.
[18] R. Verfürth, A Review of A Posteriori Error Estimation and Adaptive Mesh-Refinement Techniques, Wiley–Teubner, Chichester, 1996.
[19] O.C. Zienkiewicz, J.Z. Zhu, The superconvergent patch recovery and a posteriori error estimates, Int. J. Numer. Methods Eng. 33 (1992) 1331–1364.